Biochimica et Biophysica Acta 1828 (2013) 2238–2246

Contents lists available at SciVerse ScienceDirect

Biochimica et Biophysica Acta

journal homepage: www.elsevier.com/locate/bbamem

Large scale production of the active human ASCT2 (SLC1A5) transporter in *Pichia pastoris* — functional and kinetic asymmetry revealed in proteoliposomes

Piero Pingitore [a,b], Lorena Pochini [a], Mariafrancesca Scalise [a], Michele Galluccio [a], Kristina Hedfalk [b], Cesare Indiveri [a,*]

[a] Department BEST (Biologia, Ecologia, Scienze della Terra) Unit of Biochemistry and Molecular Biotechnology, University of Calabria, Via P. Bucci 4c, 87036 Arcavacata di Rende, Italy
[b] Department of Chemistry and Molecular Biology, University of Gothenburg, PO Box 462, SE-405 30 Göteborg, Sweden

ARTICLE INFO

Article history:
Received 13 April 2013
Received in revised form 28 May 2013
Accepted 31 May 2013
Available online 10 June 2013

Keywords:
Transport
Over-expression
Purification
Liposomes

ABSTRACT

The human glutamine/neutral amino acid transporter ASCT2 (hASCT2) was over-expressed in *Pichia pastoris* and purified by Ni^{2+}-chelating and gel filtration chromatography. The purified protein was reconstituted in liposomes by detergent removal with a batch-wise procedure. Time dependent [^{3}H]glutamine/glutamine antiport was measured in proteoliposomes which was active only in the presence of external Na^+. Internal Na^+ slightly stimulated the antiport. Optimal activity was found at pH 7.0. A substantial inhibition of the transport was observed by Cys, Thr, Ser, Ala, Asn and Met (≥70%) and by mercurials and methanethiosulfonates (≥80%). Heterologous antiport of [^{3}H]glutamine with other neutral amino acids was also studied. The transporter showed asymmetric specificity for amino acids: Ala, Cys, Val, Met were only inwardly transported, while Gln, Ser, Asn, and Thr were transported bi-directionally. From kinetic analysis of [^{3}H]glutamine/glutamine antiport Km values of 0.097 and 1.8 mM were measured on the external and internal sides of proteoliposomes, respectively. The Km for Na^+ on the external side was 32 mM. The homology structural model of the hASCT2 protein was built using the GltPh of *Pyrococcus horikoshii* as template. Cys395 was the only Cys residue externally exposed, thus being the potential target of SH reagents inhibition and, hence, potentially involved in the transport mechanism.

1. Introduction

Amino acid transport systems play the pivotal role of maintaining the amino acid homeostasis in mammalian cells. Among many transporters involved in this function there is a group which shares specificity for glutamine, thus playing the role of mediating glutamine trafficking in different tissues and intestinal and renal (re)absorption [1–3]. A lot of functional data have been obtained by studying the transporters in cell systems such as cancer cell lines or *Xenopus laevis* oocytes. Thus the glutamine-specific transporters have been firstly classified on the functional basis. More recently the various transporters have been assigned to different protein families (SLC) on the basis of gene and primary structure analysis. Taking into account both types of classifications, the glutamine-specific transporters can be divided in sodium-dependent systems: system ASC/ATB0 (SLC1), system $B^{0,+}$ (SLC6), system y + L (SLC7), system N and A (SLC38) and sodium-independent systems: system L (SLC7) and system $b^{0,+}$ (SLC6). Some transporters can be further distinguished in tolerant (N and y + L) or not tolerant (ASCT2) for the substitution of Na^+ by Li^+ or sensitivity towards inhibitors such as MeAIB (system A) or BCH (System L, LAT1) [1–3]. However, several functional properties of the amino acid transporters remain unknown or controversial, due to some limitations of the cell experimental models given by the contemporary presence of similar transport systems and/or enzymes which could affect the transport assays and by the difficult access to the internal side. Most of these problems can be overcome using simpler models for studying transport, such as the proteoliposome experimental system which revealed suitable for studying functional and kinetic properties of transporters [4,5]. Concerning the structure of mammalian amino acid transporters no crystallographic data is available so far. High resolution structures have only been achieved for some

Abbreviations: MeAIB, a-(methylamino)isobutyric acid; BCH, 2-aminobicyclo-(2,2,1)-heptane-2-carboxylic acid; $C_{12}E_8$, octaethylene glycol monododecyl ether; YPDS, Yeast Extract Peptone Dextrose Sorbitol; BMGY, Buffered Glycerol-complex Medium; DDM, n-dodecyl-beta-D-maltoside; LDAO, n-dodecyl-N,N-dimethylamine-N-oxide; CHAPS, 3-((3-cholamidopropyl)dimethylammonium)-1-propanesulfonate; p-OHMB, p-hydroxymercuribenzoate; MTSET, 2-(trimethylammonium)ethyl methanethiosulfonate, Bromide; MTSEA, 2-aminoethyl methanethiosulfonate hydrobromide; NEM, N-ethylmaleimide; PEM, N-phenylmaleimide; PLP, pyridoxal-5-phosphate; DEPC, diethyl pyrocarbonate

* Corresponding author. Tel.: +39 0984 492939; fax: +39 0984 492911.
E-mail addresses: piero.pingitore@alice.it (P. Pingitore), lorena.pochini@unical.it (L. Pochini), mariafrancesca.scalise@unical.it (M. Scalise), michele.galluccio@unical.it (M. Galluccio), kristina.hedfalk@chem.gu.se (K. Hedfalk), cesare.indiveri@unical.it (C. Indiveri).

0005-2736
http://dx.doi.org/10.1016/j.bbamem.2013.05.034

bacterial homologues of amino acid transporters [6,7]. On the basis of these structures, homology models have been obtained for mammalian amino acid transporters, some of which have been in part validated by chemical targeting [8–10]. Very interestingly the expression of some of the transporters responsible for glutamine trafficking is up-regulated in tumors [2]. Cancer cells, in fact, require high amounts of glutamine for energy and growth purposes [2,11]. In this scenario it becomes clear that the study of glutamine transporters is a hot research topic and strategies for over-expressing the transporters in large scale and studying their structure/function relationships are very welcome. Among the most interesting transporters in human physiology and pathology there is the Na^+-dependent glutamine/neutral amino acid transporter ASCT2 (SLC1A5) previously known in humans as ATB0. This transport system has been identified in human cell systems even though the kinetic properties and substrate specificity are not fully understood [2,3,12] while the rodent isoform, besides being studied in cell systems [13–16], has been also functionally and kinetically characterized in proteoliposomes [9,17,18]. Basic functional and kinetic parameters of the kidney rat protein determined in both experimental models correlated well. Novel functional properties such as the ATP regulation, the internal side Km, the reaction mechanism, and the pH dependence of glutamate transport were revealed using proteoliposomes [17,18]. Due to its over-expression in cancer cells, ASCT2 has been proposed as a potential target for antitumor drugs [2]. Very recently, a molecular screening of ditiazoles, potent inhibitors of the rat ASCT2, has been carried out in proteoliposomes [19]. These results highlighted the importance of obtaining the recombinant human ASCT2 for performing structural, functional and inhibition studies. In this work, the high level production of the human ASCT2 in *Pichia pastoris* is described. The function of the transporter extracted from yeast membranes has been assayed in proteoliposomes where the protein has been inserted in a right-side-out orientation (see Discussion) with respect to the cell membrane, thus constituting a suitable tool for unequivocal functional characterization and interaction studies with potential drugs.

2. Materials and methods

2.1. Materials

The *P. pastoris* wild type strain (X-33), the pPICZB vector, NuPAGE® 4–12% Bis-Tris Gels were purchased from Invitrogen; restriction endonucleases and other cloning reagents from Fermentas; PD-10 columns, Superdex 200 10/300 GL, ÄKTA FPLC system, ECL plus, Hybond ECL membranes and L-[^{3}H]glutamine from GE Healthcare; Ni-NTA agarose and polypropylene columns from Qiagen, anti His_6 antibody from Clontech; the anti mouse IgG HRP conjugate from Promega; $C_{12}E_8$ from Anatrace; Amberlite XAD-4, egg yolk phospholipids (3-sn-phosphatidylcoline from egg yolk), Sephadex G-75, L- glutamine and all the other reagents were from Sigma-Aldrich.

2.2. Cloning of hASCT2

The wild type gene was isolated from total RNA of primary human fibroblasts by reverse transcription. Initially, the 1623 bp cDNA encoding hASCT2 (GenBank NM_005628.2, SLC1A5) was amplified using the forward primer *Nde*I-hASCT2: 5′-G GAA TTC CAT ATG GTG GCC GAT CCT CCT CG-3′ and the reverse primer *Hind*III-hASCT2: 5′-CCC AAG CTT TTA CAT GAC TGA TTC CTT CTC-3′, respectively. The amplified cDNA sequence was verified by sequencing using the ABI 310 automated sequencer Applied Biosystems. For subsequent cloning to *P. pastoris*, the full length cDNA coding for hASCT2 was amplified using the forward primer *Eco*RI-hASCT2: 5′-ATA CCG GAA TTC **AAA ATG G**TT GCC GAT CCT CCT CGA GAC TCC-3′ and the reverse primer *Xba*I-hASCT2: 5′-A TAC TAG TCT AGA TCA ATG ATG ATG ATG ATG ATG CAT GAC TGA TTC CTT CTC AGA GGC-3′, coding a C-terminal His_6 tag. Restriction sites are underlined and the Kozak consensus sequence is shown in bold.

The hASCT2 gene was codon optimized for *P. pastoris* by GenScript and the artificial cDNA included a 5′ *Eco*RI restriction site plus the Kozak consensus sequence and a 3′ *Xba*I restriction site plus a C-terminal His_6 fusion tag. In the optimized gene, the Codon Adaptation Index (CAI) [20] was upgraded from 0.51 (wild type) to 0.82 (optimized) and the GC content was decreased from 63.01% to 45.43%. For cloning in *P. pastoris* both the wild type gene (wt-hASCT2) and the optimized gene (Opt-hASCT2) were inserted in the *Eco*RI/*Xba*I sites of the pPICZB expression vector, resulting in two different recombinant constructs, defined as pPICZB-(wt)hASCT2-His_6 and pPICZB-(Opt)hASCT2-His_6. Both constructs were verified by sequencing.

2.3. Recombinant production of hASCT2

To obtain the recombinant hASCT2-His_6 protein, the resulting plasmids were linearized with *Pme*I and the transformation into the *P. pastoris* wild type strain X-33 was performed by electroporation [21]. To select putative multi-copy recombinants a total of 52 transformants for each construct were tested for growth on YPDS plates containing 2000 μg/mL Zeocin and analyzed after 3 days. Small-scale production was performed in triplicates in shake flask cultures as previously described [22]. For large scale protein production, *P. pastoris* strains producing recombinant hASCT2 (X33/pPICZB-(wt)hASCT2-His_6 and X33/pPICZB-(Opt)hASCT2-His_6) were grown at 30 °C in a 3 L fermentor (Infors HT) having an Initial Fermentation Volume (IFV) of 1.5 L basal salt medium [23] containing 6.53 mL PTM1 trace salts [24]. An overnight pre-culture of 75 mL in BMGY having an OD_{600} of about 4 was used to inoculate the fermentor. The initial glycerol volume was consumed after approximately 24 h and the culture was fed with 150 mL 50% glycerol (v/v) for 24 h to increase biomass. To induce production of recombinant hASCT2, the culture was fed with 150 mL methanol for 48 h. To obtain the membrane fraction, *P. pastoris* cells overproducing hASCT2 were resuspended in buffer A (50 mM Tris, pH 7.4, 150 mM NaCl, 6 mM β-mercaptoethanol and 0.5 mM PMSF) at a concentration of about 1 g/mL. Droplets of the cell suspension were frozen in liquid nitrogen and cells were broken by an X-Press (four passages). The suspension was centrifuged at 6000 *g* for 30 min and the supernatant containing membrane and cytosolic fractions (crude extract) was collected. This supernatant was ultracentrifuged in a Ti45 rotor at 140,000 *g* for 1 h. The resulting membrane pellet was washed with urea buffer (5 mM Tris pH 7.4, 2 mM EDTA, 2 mM EGTA and 4 M urea) and then again ultracentrifuged as above. The washed membrane fractions (pellet) containing (wt)hASCT2 or (Opt)hASCT2 were resuspended in buffer B (25 mM Tris, pH 7.4, 250 mM NaCl, 6 mM β-mercaptoethanol and 10% glycerol) at a final concentration of about 300 mg/mL and homogenized using a handheld electric homogenizer. Aliquots of 6 mL of the membrane fraction were stored at −80 °C. Various stages from the protein purification procedure were analyzed by SDS-PAGE and immunoblot.

2.4. Solubilization and purification of hASCT2

For large-scale solubilization and purification (Opt)-hASCT2, about 1.5 g of washed membranes (300 mg/mL) was resuspended in buffer B containing 1% $C_{12}E_8$ (w/w) to a concentration of 150 mg/mL and gently mixed by agitation for 3 h at 4 °C. After solubilization, the solubilized material was centrifuged at 120,000 *g* for 1 h, imidazole (50 mM) was added to the supernatant which was mixed with 3 mL Ni-nitrilotriacetic acid (NTA) agarose resin equilibrated with the equilibration buffer (20 mM Tris pH 7.4, 300 mM NaCl, 10% glycerol, 6 mM β-mercaptoethanol, 0.03% $C_{12}E_8$, and 50 mM imidazole) and incubated by gentle agitation for 3 h at 4 °C. The Ni-NTA resin was subsequently packed into a plastic 1 mL column. The resin was washed with 30 mL of the equilibration buffer. Then, 4 mL of the

same buffer containing 300 mM imidazole and 2 mL of the same buffer containing 500 mM imidazole (referred as elution buffers) were added. Fractions of 1 mL were collected; fractions 2–4 were pooled and desalted on a PD-10 desalting column pre-equilibrated with desalting buffer (20 mM Tris pH 7.4, 100 mM NaCl, 10% glycerol, 6 mM β-mercaptoethanol and 0.03% $C_{12}E_8$), from which 3.5 mL was collected. Desalted protein was concentrated to 250 μL by vacuum Vivaspin 30 K spin concentrator and loaded onto a Superdex 200 10/300 GL column pre-equilibrated with desalting buffer, and eluted with the same buffer using the ÄKTA FPLC system. Fractions of 500 μL were collected and analyzed by SDS-PAGE. The total protein concentration of each fraction was determined by Bradford protein assay using bovine serum albumin (BSA) as a standard (Bio-Rad DC Protein assay). Protein samples were analyzed by precasted SDS-PAGE on NuPAGE® 4–12% Bis-Tris Gels under reducing conditions with 20 mM DTT. The gel was stained with SimplyBlue™ SafeStain (Invitrogen). Immonoblotting analysis was performed using anti-His_6 antibody 1:5000. To verify the identity of the recombinant protein the purified fraction was analyzed by SDS-PAGE, the band of interest excises and analyzed by mass spectrometry as previously described [25].

2.5. Reconstitution of the hASCT2 into liposomes

The purified hASCT2 was reconstituted by removing the detergent using the batch-wise method. In this procedure, the mixed micelles containing detergent, protein and phospholipids were incubated with 0.5 g Amberlite XAD-4 resin under rotatory stirring (1400 rev/min) at room temperature (25 °C) for 40 min [26]. The composition of the initial mixture used for reconstitution was: 100 μL of the solubilized protein (5 μg protein), 120 μL of 10% $C_{12}E_8$, 100 μL of 10% egg yolk phospholipids (w/v) in the form of sonicated liposomes prepared as previously described [5], 10 mM L-glutamine, and 20 mM Tris/HCl pH 7.0 (except where differently specified) in a final volume of 700 μL. All the operations were performed at 4 °C.

2.6. Transport measurements

To remove the external substrate for uptake experiments, 600 μL of proteoliposomes was passed through a Sephadex G-75 column (0.7 cm diameter × 15 cm height) preequilibrated with 20 mM Tris/HCl pH 7.0 and sucrose at an appropriate concentration to balance the internal osmolarity. Transport (uptake) measurement was started by adding 50 μM [^{3}H]glutamine and 50 mM Na-gluconate (except where differently specified) to the proteoliposomes. For efflux measurements, proteoliposomes (600 μL), containing 10 mM glutamine, were preloaded with radioactivity by transporter-mediated exchange equilibration [27] by incubation with 50 μM [^{3}H]glutamine at high specific radioactivity (2 μCi/nmol) and 50 mM Na-gluconate for 120 min at 25 °C. External compounds were removed by another passage of the proteoliposomes through Sephadex G-75 as described above. Transport (efflux) measurement was started by adding non radioactive substrates to the preloaded proteoliposomes. In both uptake and efflux assays, transport was stopped by adding 10 μM mersalyl at the desired time interval. In control samples, the inhibitor was added at time zero according to the inhibitor stop method [28]. The assay temperature was 25 °C. At the end of the transport assay, each sample of proteoliposomes (100 μL) was passed through a Sephadex G-75 column (0.6 cm diameter × 8 cm height) to separate the external from the internal radioactivity. Liposomes were eluted with 1 mL 50 mM NaCl and collected in 4 mL of scintillation mixture, vortexed and counted. For the determination of [^{3}H]glutamine uptake, the experimental values were corrected by subtracting the respective controls (samples inhibited at time zero); the initial rate of transport was measured by stopping the reaction after 10 min, i.e., within the initial linear range of [^{3}H]glutamine uptake into the proteoliposomes. For the determination of [^{3}H]glutamine efflux the experimental values at each time were subtracted from the radioactivity initially present in the proteoliposomes at time zero. Fitting of experimental data in a first order rate equation to obtain rate constants was performed using the non linear regression analysis Grafit software (version 5.0.13).

To measure the specific activity of hASCT2, the amount of reconstituted recombinant protein was estimated from Coomassie blue stained SDS-PAGE gels by using the Chemidoc imaging system equipped with Quantity One software (Bio-Rad) as previously described [29].

2.7. Homology modeling of hASCT2

The homology structural model of the hASCT2 was built using the glutamate transporter homologue from *Pyrococcus horikoshii* crystal structure (1XFH) as template. The amino acid sequence of the rat ASCT2 (NP_786934) and the glutamate transporter (NP_143181) was aligned manually using ClustalW as described in Ref. [6] and adjusted for hASCT2, belonging to the same family of glutamate and neutral amino acid transporters as rASCT2. The optimized alignment was used to run the program Modeller 9.11 [30].

3. Results

3.1. Over-production and purification of hASCT2

To identify high producing *P. pastoris* clones, a high zeocin screen was performed followed by a small scale production test in 25 mL cultures to verify proper membrane localization of recombinant hASCT2 (data not shown). From these tests, the positive clones for the following large scale production were obtained. To achieve higher production levels of (wt)hASCT2 and (Opt)hASCT2 (obtained by the cDNA optimized for *P. pastoris*, coding the same hASCT2 protein as the wt cDNA), the growth was scaled up in a 3 L fermentor to supply the high oxygen demand of *P. pastoris*. Cultivating X-33/(wt)hASCT2 and X-33/(Opt)hASCT2 under tightly controlled regimes resulted in a total cell mass of 350 g wet weight.

Under this culture condition high yields of an over-produced protein with an apparent molecular mass of about 50 kDa were observed both in the X-33/(wt)hASCT2 and X-33/(Opt)hASCT2 (Fig. 1A). The protein was identified as the hASCT2 in crude extract and membrane fractions by immunoblotting using an anti-His antibody (Fig. 1B). The yield of (Opt)hASCT2 was more than two-fold as compared to the (wt) hASCT2. Thus, in all the experiments hASCT2 from X-33/(Opt)hASCT2 was used. One or two higher molecular mass bands were detected by the immunostaining, corresponding to double and triple apparent molecular mass of the hASCT2 monomer (Fig. 1B).

Before purification, a solubilization trial was carried out on the membrane fraction to find a suitable detergent. Nine different detergents (Cholate, DDM, Brij35, LDAO, β-octylglucoside, CHAPS, Fos-choline-12, Triton X-100, $C_{12}E_8$) were tested. DDM, LDAO, Fos-choline-12 and $C_{12}E_8$ showed the best efficiency in solubilizing hASCT2 (not shown), although only $C_{12}E_8$ revealed to be suitable for protein reconstitution in liposomes (see below). For large scale purification, urea washed membranes extracted from the X33/(Opt)hASCT2 were solubilized with 1% $C_{12}E_8$. The solubilized protein (Fig. 2A lane 1) was incubated with the Ni-NTA agarose resin. After washing, virtually all the unbound proteins were removed and most of the protein was found in fractions 2–4 after elution (1 ml each) in 300 mM imidazole (Fig. 2A lanes 3–5). The addition of the same elution buffer containing 500 mM imidazole led to a further recovery of small amounts of hASCT2 as observed in fractions 5–6 (Fig. 2A, lanes 6–7). The purified fractions contained a 50 kDa protein besides the two higher molecular mass bands corresponding to dimeric and trimeric forms of the protein which were verified by the immunoblot (Fig. 2B). To confirm the correspondence of the purified bands with the hASCT2 protein, mass spectrometry analysis was also performed. Only peptides containing the hASCT2 sequence (Table 1) were recognized after trypsin treatment of

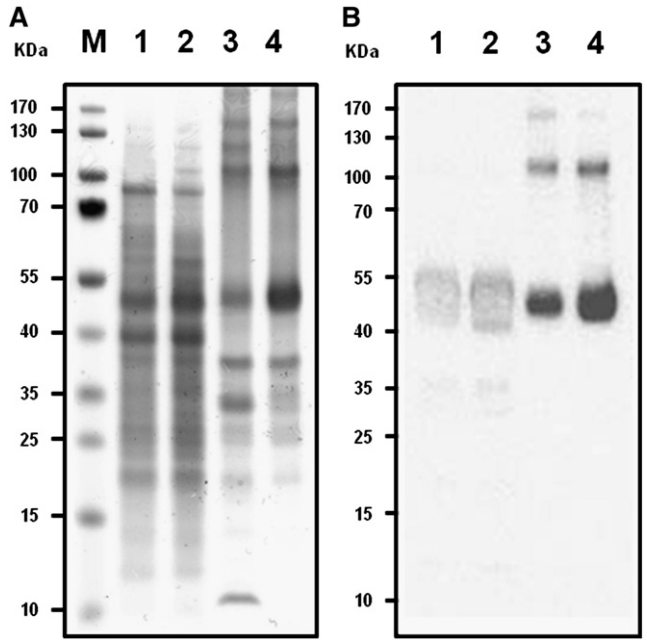

Fig. 1. Production of (wt)hASCT2 and (Opt)hASCT2 using fermentor growth. (A) SDS-PAGE (4–12%) gel electrophoresis analysis of the hASCT2 production stained as described in Materials and methods. M: protein markers; lanes 1–2, crude extract from *P. pastoris* cells producing (wt)hASCT2 (lane 1) or (Opt)hASCT2 (lane 2) in the fermentor; lanes 3–4: membrane fraction from *P. pastoris* cells producing (wt)hASCT2 (lane 3) or (Opt)hASCT2 (lane 4) in the fermentor. In each lane 10 μg total protein was loaded. (B) Immunoblot using an anti-His antibody showing hASCT2 production of the same protein fractions as in (A). In lanes 1 and 2, 50 μg total protein was loaded, in lanes 3 and 4, 1 μg total protein was loaded.

the 50 kDa and the other higher molecular mass bands present in the purified fraction (Fig. 2). These higher molecular mass bands of hASCT2 are probably formed by monomers tightly interacting or covalently cross-linked and could not be dissolved by SDS. Protein fractions

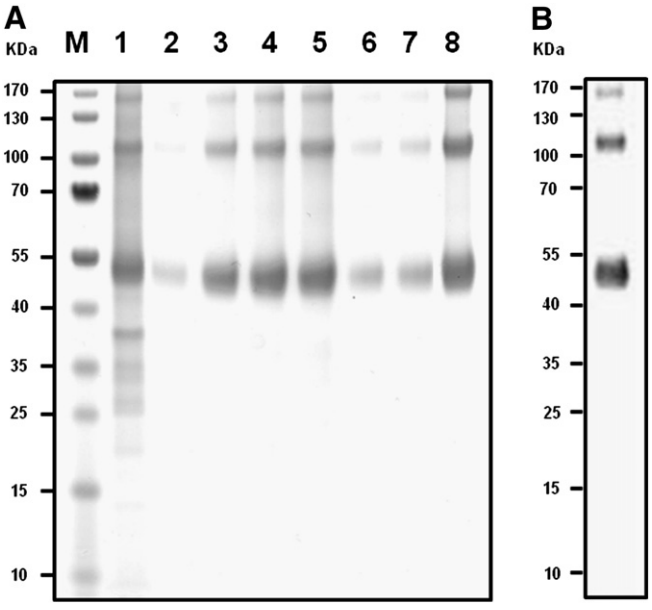

Fig. 2. Purification of (Opt)hASCT2. (A) SDS-PAGE (4–12%) gel electrophoresis analysis of the (Opt)hASCT2 purification stained as described in Materials and methods. M: protein markers; lane 1: membrane fraction from *P. pastoris* cells producing (Opt)hASCT2 in the fermentor (10 μg) solubilized with 1% $C_{12}E_8$; lanes 2–5: fractions 1–4 from Ni-NTA affinity chromatography eluted with 300 mM imidazole elution buffer; lanes 6–7: fractions 5–6 from Ni-NTA affinity chromatography eluted with 500 mM imidazole elution buffer; lane 8: pooled purified fractions 2–4 after desalting on PD10 column. (B) Immunoblot of purified protein on lane 8 using an anti-His antibody.

Table 1
Mass values and amino acid sequence obtained by mass spectrometry analysis of the tryptic peptides of recombinant hASCT2.

Peptide mass (Da)	Sequence position	Peptide sequence
984.51	2–10	VADPPRDSK[a–c]
1277.67	179–189	EVLDSFLDLAR[a]
1135.49	203–211	SYSTTYEER[a–c]
1096.64	248–257	LGPEGELLIR[a,b]
1062.49	363–372	CVEENNGVAK[a]
1143.62	493–502	STEPELIQVK[a–c]
1102.54	526–537	GPAGDATVASEK[a–c]
1133.52	363–372	cVEENNGVAK[a–c]
801.39	1–7	mVADPPR[a–c]
1131.55	1–10	mVADPPRDSK[a–c]

m: oxidation.
c: propionamide.
[a] Peptides from monomer.
[b] Peptides from dimer.
[c] Peptides from trimer.

with apparent monomeric molecular mass on SDS-PAGE could be isolated from the higher molecular mass products by size exclusion chromatography using a Superdex 200 column (Fig. 3). However, most of the oligomeric forms of hASCT2 were eluted in the fractions corresponding to the void volume (lanes 1–3) of the column or to very high molecular masses (lanes 4–7), indicating that these protein forms were mostly super-aggregated. While, most of the protein with apparent molecular mass of 50 kDa on SDS-PAGE (Fig. 3 lanes 8–11) eluted in the fractions corresponding to about150 kDa, indicating that the non-aggregated protein was most likely in a trimeric form before SDS treatment. The final protein yield after the purification procedure was estimated to be 10 mg per liter of cell culture.

3.2. Optimization of the reconstitution

The reconstitution procedure previously established for the rASCT2 [17] was not effective as it is, for reconstituting the hASCT2. The procedure of detergent removal had to be changed from cyclic column passages to batch-wise procedure to prolong the time of incubation of the reconstitution mixture with the hydrophobic resin. Moreover, some parameters which are known to be critical for the detergent removal reconstitution method had to be modified. The detergent/lipid ratio was increased from 0.95 (w/w), used for the rat protein, to 1.2 (w/w); while the amount of protein in the reconstitution mixture was reduced from 30 to 5 μg.

3.3. Functional characterization

The time dependence of the transport activity was measured as 50 μM [^{3}H]glutamine uptake in proteoliposomes, under different conditions (Fig. 4A). The uptake of [^{3}H]glutamine in the presence of external Na^+ into the proteoliposomes containing internal glutamine, increased as function of the time up to 90 min i.e., when the radioactivity equilibrium was reached; if Na^+ was present also inside the proteoliposomes a stimulation of the uptake was observed. On the contrary, no [^{3}H]glutamine uptake was detected in the absence of external Na^+ even in the presence of internal Na^+. Moreover, nearly no [^{3}H]glutamine uptake could be detected into vesicles without internal substrate or with lower internal glutamine concentration (50 μM) even in the presence of internal Na^+ (Fig. 4A). No transport was observed in proteoliposomes reconstituted with boiled protein, demonstrating that glutamine antiport was mediated by the hASCT2 protein. The experimental data fitted a first order rate equation from which a rate constant, k, of 0.039 min^{-1} and a transport rate (the product of k and the transport at equilibrium) of 4.67 $nmol \cdot min^{-1} \cdot mg\ protein^{-1}$ were calculated in the absence of internal Na^+; in its presence a rate constant, k, of 0.0279 min^{-1}

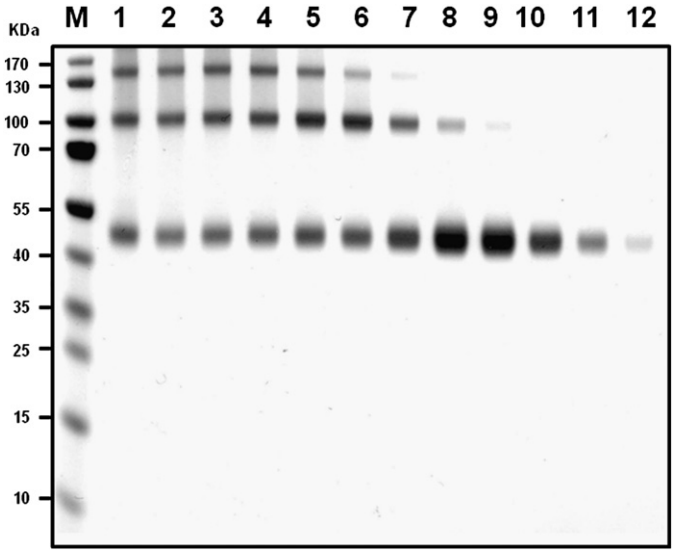

Fig. 3. SDS-PAGE analysis of (Opt)hASCT2 size exclusion chromatography. A total of 250 μL of desalted purified hASCT2 was loaded onto a Superdex 200 size exclusion column and eluted with 20 mM Tris pH 7.4, 100 mM NaCl, 10% glycerol, 6 mM β-mercaptoethanol and 0.03% $C_{12}E_8$. Fractions of 0.5 mL were collected and analyzed by SDS-PAGE (4–12%). M: protein markers; lanes 1–12 protein fractions from 8 mL to 14 mL volume column. Fractions 8–11 correspond to a molecular mass of about 150 kDa according to standard calibration of the column manufacturer.

and a transport rate of 5.0 nmol·min^{-1}·mg protein^{-1} were calculated. Fig. 4B shows the effects of different concentrations of intraliposomal Na^+. The stimulation of transport was maximal at 20 mM (40 mOsM) internal Na^+ and did not increase at higher concentration. No stimulation was observed if Na^+ was substituted by K^+ or by sucrose, indicating that the observed effect was specifically exerted by Na^+. The dependence of the glutamine antiport on the pH has been studied (Fig. 5). Maximal transport activity was observed at pH 7.0. At more acidic or alkaline pH the activity drastically decreased.

3.4. Amino acid and inhibitor specificity

The effect of externally added amino acids on the glutamine antiport was analyzed (Fig. 6). Cysteine, threonine, serine, alanine, and asparagine, were the most efficient in inhibiting the transport with more than 80% inhibition at amino acid concentration of 1 mM. Inhibition between 70 and 40% was exerted by methionine, valine and leucine. The extent of inhibition decreased to less than 40% for tyrosine and less than 20%, or insignificant, for the other amino acids. The amino acid analog MeAIB and BCH did not inhibit at all the transporter (Fig. 6). The sensitivity to chemical compounds known to interact with specific amino acid residues of proteins was also investigated (Fig. 7). The SH reagents $HgCl_2$, mersalyl and pOHMB were the most potent inhibitors, followed by methanethiosulfonates, while maleimides (NEM, PEM) and the NH_2 reagent PLP had lower inhibitory effects. The histidine reagent DEPC did not exert any inhibitory effect on [^{3}H]glutamine uptake. To establish which of the amino acids could be transported by the antiport reaction catalysed by the reconstituted hASCT2, the experiments of Fig. 8 have been performed. [^{3}H]glutamine uptake was measured in proteoliposomes containing different amino acids as counter substrates. Serine, asparagine and threonine efficiently stimulated [^{3}H]glutamine uptake, i.e., were transported by ASCT2 as efflux substrates from the intraliposomal compartment. Surprisingly, alanine and cysteine, even though revealed to be good inhibitors of [^{3}H]glutamine uptake, could not be transported (Fig. 8A), as well as valine, methionine, histidine, glutamate and arginine, tested among the non-inhibiting amino acids; the same results were obtained when 20 mM internal Na^+ was present (not shown). Alternatively, [^{3}H]glutamine efflux from prelabeled proteoliposomes was measured in the

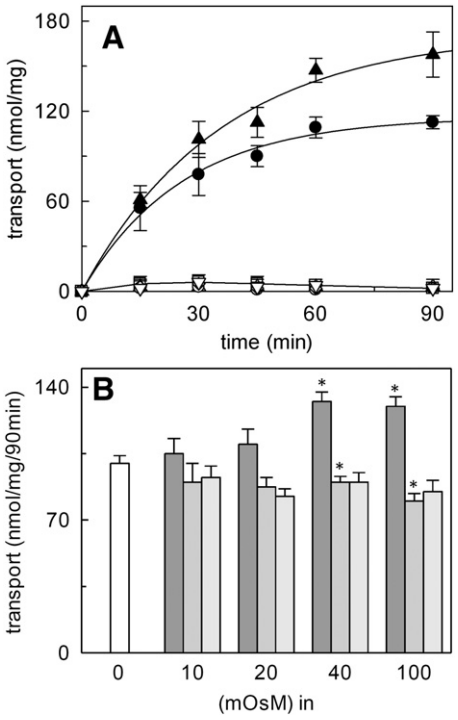

Fig. 4. [^{3}H]glutamine uptake by hASCT2 reconstituted in proteoliposomes: effects of external and internal Na^+. (A) The reconstitution was performed as described in Materials and methods. Transport was started by adding 50 μM [^{3}H]glutamine at time zero to proteoliposomes reconstituted with hASCT2 (●,□, Δ) or with protein treated for 20 min at 100 °C (○), in the absence (□, ◇) or presence (●,○, Δ, ▲, ◇) of 50 mM external Na-gluconate; 10 mM glutamine (●, ○, □, ▲, ◇), 50 μM glutamine (◇) or no internal substrate (Δ) was present inside the proteoliposomes. In (◇, ◇) 20 mM internal Na-gluconate was present. The transport reaction was stopped at the indicated times, as described in Materials and methods. Results are means ± S.D. from three experiments. (B) The reconstitution was performed as described in the Materials and methods except that Na^+-gluconate (dark bars), and K-gluconate (gray bars) were added into proteoliposomes at the concentrations: 5, 10, 20 and 50 mM; light gray bars indicates intraliposomal sucrose at concentrations: 10, 20, 40, 100 mM; white bar, no additions. Transport was started by adding 50 μM [^{3}H]glutamine at time zero to proteoliposomes together with extraliposomal 50 mM Na^+-Gluconate. The transport reaction was stopped at 90 min, as described in Materials and methods. Results are means ± S.D. from three experiments. *Significantly different from sample without added inhibitor as estimated by Student's *t* test ($P < 0.05$).

presence of externally added amino acids (Fig. 8B). Serine, asparagine, threonine, alanine and cysteine revealed to strongly stimulate efflux of [^{3}H]glutamine, i.e. could be inwardly transported in antiport with glutamine. Valine and methionine were also inwardly transported

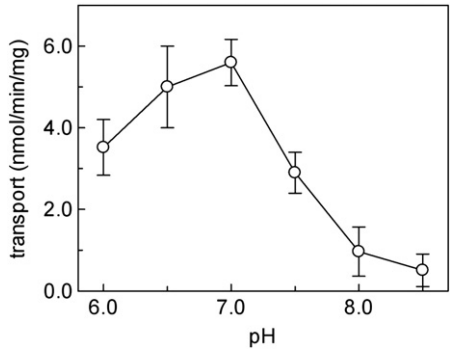

Fig. 5. Effect of pH on hASCT2 transport activity. The reconstitution was performed as described in Materials and methods except that 20 mM Tris/HCl at the indicated pH was used. Transport was started by adding 50 μM [^{3}H]glutamine in 20 mM Tris/HCl at the indicated pH to proteoliposomes containing 10 mM glutamine, in the presence of 50 mM external Na-gluconate. Results are means ± S.D. from three experiments.

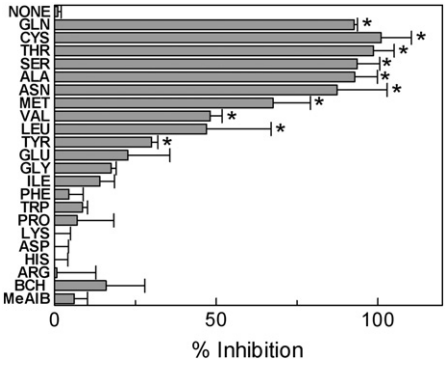

Fig. 6. Effect amino acids and substrate analogs on hASCT2 transport activity. The reconstitution was performed as described in Materials and methods. Transport was started by adding 50 μM [^{3}H]glutamine to proteoliposomes containing 10 mM internal glutamine, in the presence of 50 mM external Na-gluconate. The molecules were added 1 min before the labeled substrate at the concentration 1 mM. Percentage of inhibition was calculated for each experiment with respect to the sample without added inhibitor. Results are means ± S.D. from three experiments. *Significantly different from sample without added inhibitor as estimated by Student's *t* test ($P < 0.05$).

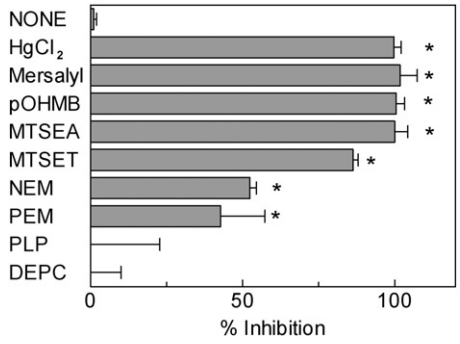

Fig. 7. Effect of protein specific reagents on hASCT2. The reconstitution was performed as described in Materials and methods. Transport was started by adding 50 μM [^{3}H]glutamine to proteoliposomes containing 10 mM internal glutamine, in the presence of 50 mM external Na-gluconate. The molecules were added 1 min before the labeled substrate at the following concentrations: 0.02 mM $HgCl_2$, mersalyl, p-OHMB; 1 mM MTSEA, MTSET, NEM or PEM; 10 mM PLP; 4 mM DEPC. Percentage of inhibition was calculated with respect to the sample without added inhibitor. Results are means ± S.D. from three experiments. *Significantly different from sample without added inhibitor as estimated by Student's *t* test ($P < 0.05$).

even though less efficiently while, histidine, glutamate and arginine were not transported.

3.5. Kinetics of ASCT2 mediated transport

The dependence of the transport rate on the glutamine concentration was studied. The initial rate of glutamine antiport (Fig. 9A) showed a dependence on the external glutamine concentration fitting the Michaelis–Menten equation, from which half-saturation constant (Km) of 0.097 ± 0.019 mM and a Vmax of 13.3 ± 1.9 nmol·min^{-1}·mg protein^{-1} (from three different experiments) were derived. A similar experiment was performed to obtain information on the intraliposomal Km, which resulted to be much higher than the external one (Fig. 9B). The measured value was 1.8 mM ± 0.52 (from three different experiments). The calculated Vmax (12.0 ± 1.5 nmol·min^{-1}·mg protein^{-1}) was similar to that measured in the experiment of Fig. 9A.

The dependence of the transport on the concentration of external cations, as gluconate salts, was studied. The data of Fig. 9C shows that the transport rate of glutamine antiport, starting from zero was strongly stimulated by external Na^+. The data could be fitted in the Michaelis–Menten equation from which a Vmax of 11.5 ± 0.57 nmol·min^{-1}·mg protein^{-1} and a Km of 32 ± 4.7 mM were calculated. The presence of Li^+ or K^+ in the extraliposomal compartment was not able to stimulate the glutamine transport.

4. Discussion

One of the major challenges concerning the study of mammalian and especially human transporters is to obtain sufficient amount of purified proteins for both structural and functional characterization. Moreover, the availability of suitable methods for transport assay is essential to characterize recombinant proteins obtained by heterologous production. Only in recent years, the number of successful over-production trials of mammalian and human transporters is slightly increasing. Over-production has been achieved using *Escherichia coli* as host, both as entire organism [31,32] or in cell free systems [33]. However, in several cases it was not possible to obtain significant levels of human proteins in bacteria, thus suggesting another host for production. This was the case for hASCT2 which was toxic to several bacterial strains screened for expression trials (data not shown). Using the yeast *P. pastoris* we succeeded in obtaining high levels of recombinant hASCT2, similar to the recently expressed hLAT2 transporter [34]. hLAT2 and hASCT2 represent the only mammalian amino acid transporters produced in yeast, so far. hASCT2 is structurally unrelated to hLAT2, but presents significant homology to glutamate transporters [6,9]. An important step for increasing the yield of recombinant hASCT2 protein was the optimization of the codons to the yeast translation machinery. Similarly, bacterial over-production of a different transporter, OCTN2, was obtained only after codon bias [35]. Noteworthy, the over-produced hASCT2 was associated to the yeast membrane

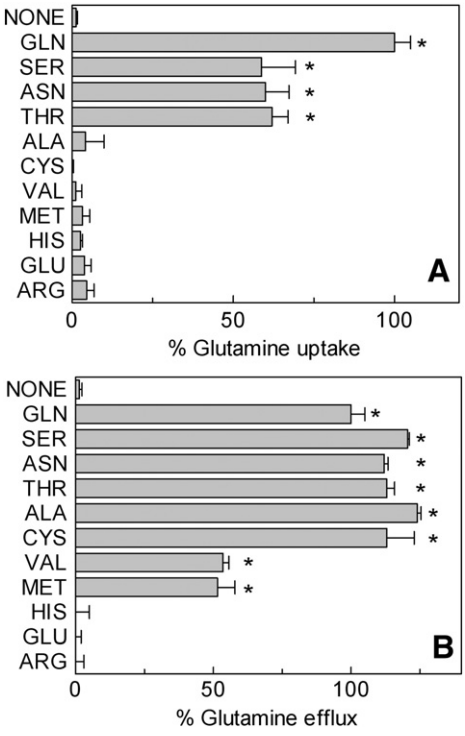

Fig. 8. Amino acids as counter substrates for hASCT2. The reconstitution was performed as described in Materials and methods. (A) The indicated substrates (10 mM) were present in the intraliposomal space (included in the reconstitution mixture). Transport was started by adding 50 μM [^{3}H]glutamine to the proteoliposomes in the presence of 50 mM external Na-gluconate. Percentage glutamine uptake was calculated for each experiment with respect to proteoliposomes containing 10 mM internal glutamine (100%). (B) Proteoliposomes were preloaded with 50 μM [^{3}H]glutamine and its efflux was measured in the presence of 10 mM of the indicated external amino acid. The efflux experiment was performed as described in Materials and methods and percentage glutamine efflux was calculated for each experiment with respect to proteoliposomes with externally added glutamine (100%). Results are means ± S.D. of the percentage of three experiments. *Significantly different from samples without internal or external substrate as estimated by Student's *t* test ($P < 0.05$).

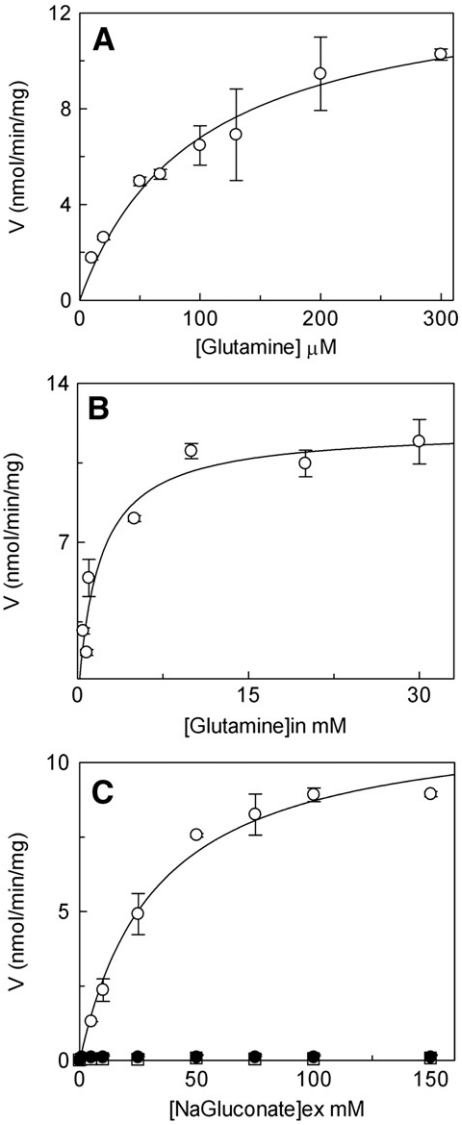

Fig. 9. Dependence of substrate concentration and the rate of glutamine antiport. The transport rate was measured adding [^{3}H]glutamine at the indicated concentration to proteoliposomes containing 10 mM internal glutamine (A) or 200 μM [^{3}H]glutamine to proteoliposomes containing internal glutamine at the indicated concentrations (B), in the presence of 50 mM external Na-gluconate in 10 min; in (C) transport rate was measured adding 50 μM [^{3}H]glutamine to proteoliposomes containing 10 mM glutamine in the presence of the indicated concentrations of Na-gluconate (○), K-gluconate (●) or Li-acetate (□) in 10 min. Data were plotted according to Michaelis–Menten equation. Results are means ± S.D. of three experiments.

fraction indicating proper folding of recombinant hASCT2. The preferred detergent for solubilization, $C_{12}E_8$, was proven by the functional characterization and correlated well with previous studies conducted on the rASCT2 solubilized in its active form from rat kidney membranes [17]. Moreover, the purified hASCT2 was eluted from Superdex 200 chromatography as a 150 kDa oligomeric form suggesting that the protein tends to form trimers. This observation is in agreement with the data obtained on the GltPh transporter of *P. horikoshii* [6] and to the homology structural model of rASCT2 [9].

To obtain functional information on the recombinant hASCT2 we have performed reconstitution into proteoliposomes which gives the possibility, as above mentioned, to better control several experimental conditions. Indeed, virtually all the reconstituted transporter molecules are inserted in the lipid bilayer of the liposomes with the same orientation of the native membrane (right-side-out) as suggested by the essential requirement of external Na^+ for transport (Fig. 9C), which correlates with the presence of Na^+ in the extracellular compartment; accordingly, single Km values are observed both outside and inside. Similar orientation was previously found for other reconstituted transporters [4,17,26,36]. However, definitive proofs of protein orientation will be given by structure/function relationship studies. The unidirectional insertion of transport proteins in the membrane is probably guaranteed by the slow process of proteoliposome formation starting from mixed micelles or destabilized liposomes. The insertion of the protein into the bilayer is also influenced by the asymmetrical structure of the protein itself together with the small radius of the starting micelles.

The basic functional properties of the reconstituted transporter, i.e., the Na^+-dependence, intolerance for substitution of Na^+ with Li^+ and K^+, the specificity for neutral amino acids, and the lack of inhibition by the amino acid analogs MeAIB and BCH, correspond to those described in cell systems so far [3,12]. On the other hand, some important novel information on the hASCT2 has been obtained in the study presented here. In particular, besides the already documented specificity for glutamine, alanine, serine, threonine and cysteine, an asymmetric behavior with respect to the transported amino acids has been highlighted. In particular, specific amino acids such as cysteine, alanine, valine and methionine can be translocated from outside to inside of proteoliposomes, but not vice-versa. This finding suggests that hASCT2 provides cells with these amino acids exporting glutamine, threonine, serine or asparagine on the basis of metabolic needs of cells or the amino acid concentrations. At the same time, the bi-directional transport of glutamine is in agreement with the role proposed for ASCT2 in astrocytes and as a general mechanism of small amino acid reabsorption [1,14,37,38]. Also serine, asparagine and threonine are bi-directionally translocated in line with the role designed for ASCT2, together with LAT1 in the mTOR pathway which controls several cell functions [2]. It has been found that Na^+ stimulates the glutamine antiport also from the internal side to some extent, even though at a concentration higher than the intracellular Na^+ concentration. This may be explained either by sodium counter-transport, as previously found for ASCT1 [39] or by allosteric mechanism. In this work the external Km for glutamine of hASCT2 has been measured and found to be in the same range as that measured in cell systems [2,12]. Moreover, by using the proteoliposome assay, the internal Km for glutamine, so far unknown, has been determined to be twenty times higher than the external one. This reflects the difference between the extra- and intracellular concentration of glutamine and other amino acids [40]. Moreover, the difference between the external and internal Km values is in favor of the functional asymmetry of the transporter and is in agreement with the structural asymmetry of the hASCT2 protein (Fig. 10), which shows a cone-shaped form enlarged towards the extracellular side. The proteoliposome method allowed further insights in the structure–function relationship. Indeed, the reconstituted transporter, has been shown to be strongly inhibited by hydrophilic thiol specific reagents, but much less by hydrophobic ones or by the amino specific reagent PLP. These data indicates that the Cys residues involved in the observed inhibition should be located in a hydrophilic environment accessible from the extracellular space. On the basis of the homology model, Cys395 is the only Cys residue exposed towards the extracellular environment (Fig. 10), thus, it might be involved in the interaction with the hydrophilic SH reagents and inactivation of the transporter. Even though this is a speculative consideration, it correlates well with the location of Cys395 in the middle of two helical hairpins (Fig. 10 dark gray structure) whose homologues in the GltPh have been recognized as a mobile structure involved in the conformational changes allowing substrate transport [41].

By comparison with the rASCT2 some differences arose such as the Km values which are lower for hASCT2 than those of the rat counterpart, as well as the sensitivity to DEPC that inhibits rASCT2 but not the human counterpart. Moreover the hASCT2 is not regulated by intracellular ATP as observed for the rat protein. This can be explained by the

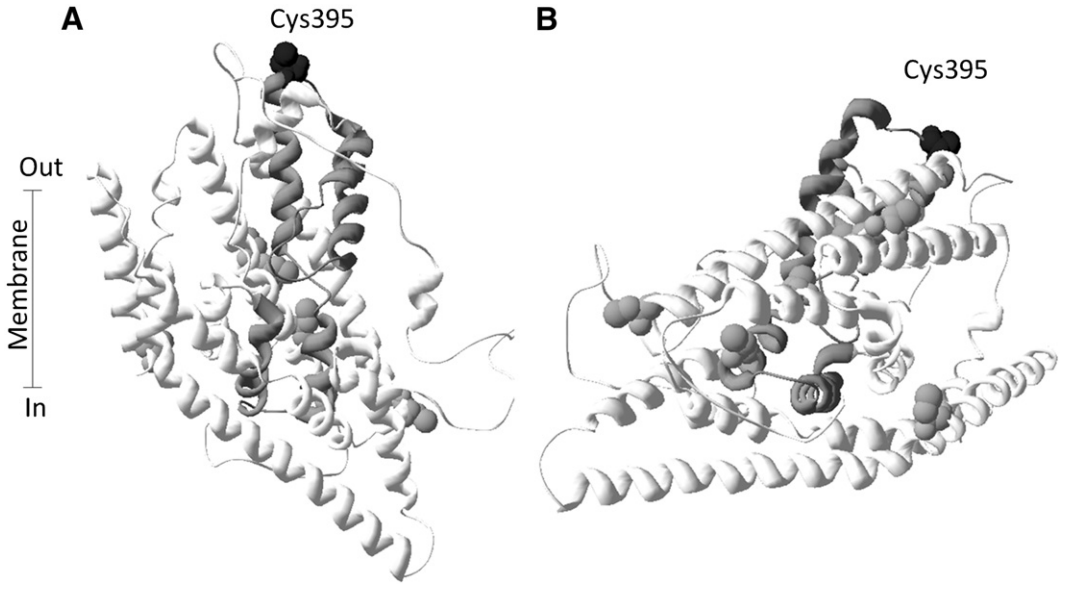

Fig. 10. Homology structural model of hASCT2. Ribbon diagram viewing the transporter from the lateral side (A) or by the intracellular side (B); Cys395 is highlighted in black. The structure homologous to the sequence segment from HP (helical hairpin) 1 to HP2 of GltPh [6,40] is highlighted in dark gray. The homology model has been represented using the molecular program SpdbViewer 4.01.

different structural properties of the human protein in comparison with the homologue protein from rat. In fact, the N-terminal sequence of the rat protein, which contains a nucleotide binding motif [17] presents some differences with respect to the human protein. Regulation of hASCT2 has been described in cell systems but no evidence of direct effectors on the activity of the transport proteins is so far presented [42–44]. Noteworthy, ASCT2 represents a potential target for cancer therapy (see Introduction). ASCT2 over-expression has been linked to the tumor suppressor pRb/E2F pathway [45]. In this context, and in line with the molecular screening on the rat isoform [19], the reconstituted hASCT2 will be very helpful for testing drugs and xenobiotics of relevance for human health. This could allow the identification of possible specific inhibitors of hASCT2 activity, in order to elicit apoptosis in cancer cells. The availability of recombinant proteins also allows site-directed mutagenesis on the human ASCT2. Applying such methods will shed further light on the involvement of hASCT2 in pathophysiology as well as in defining molecular mechanisms of transport and structural details such as the actual oligomeric form of the protein. However, only X-ray diffraction analysis of hASCT2 crystals could definitively give information on the three-dimensional structure of the transporter. The high level of production of the functional protein in a homogeneous purified fraction allows crystallographic screening for this purpose. The homology structure and, when available, the high-resolution structure will in addition be used in docking strategies for fast analysis of transporter-inhibitor interactions, which could be validated in proteoliposomes.

Acknowledgements

This work was supported by funds from: Programma Operativo Nazionale PON-ricerca e competitività 2007-2013 [PON 01_00937] “Modelli sperimentali Biotecnologici integrati per lo sviluppo e la selezione di molecole di interesse per la salute dell'uomo”, Ministero Istruzione Università e Ricerca (MIUR); European Commission, FSE funds and Calabria Region.

References

[1] M. Palacin, R. Estevez, J. Bertran, A. Zorzano, Molecular biology of mammalian plasma membrane amino acid transporters, Physiol. Rev. 78 (1998) 969–1054.
[2] B.C. Fuchs, B.P. Bode, Amino acid transporters ASCT2 and LAT1 in cancer: partners in crime? Semin. Cancer Biol. 15 (2005) 254–266.
[3] S. Broer, M. Palacin, The role of amino acid transporters in inherited and acquired diseases, Biochem. J. 436 (2011) 193–211.
[4] L. Pochini, F. Oppedisano, C. Indiveri, Reconstitution into liposomes and functional characterization of the carnitine transporter from renal cell plasma membrane, Biochim. Biophys. Acta 1661 (2004) 78–86.
[5] C. Indiveri, Studying amino acid transport using liposomes, Methods Mol. Biol. 606 (2010) 55–68.
[6] D. Yernool, O. Boudker, Y. Jin, E. Gouaux, Structure of a glutamate transporter homologue from *Pyrococcus horikoshii*, Nature 431 (2004) 811–818.
[7] L.R. Forrest, R. Kramer, C. Ziegler, The structural basis of secondary active transport mechanisms, Biochim. Biophys. Acta 1807 (2011) 167–188.
[8] S. Broer, Apical transporters for neutral amino acids: physiology and pathophysiology, Physiology (Bethesda) 23 (2008) 95–103.
[9] F. Oppedisano, M. Galluccio, C. Indiveri, Inactivation by Hg2+ and methylmercury of the glutamine/amino acid transporter (ASCT2) reconstituted in liposomes: prediction of the involvement of a CXXC motif by homology modelling, Biochem. Pharmacol. 80 (2010) 1266–1273.
[10] F. Oppedisano, L. Pochini, S. Broer, C. Indiveri, The B0AT1 amino acid transporter from rat kidney reconstituted in liposomes: kinetics and inactivation by methylmercury, Biochim. Biophys. Acta 1808 (2011) 2551–2558.
[11] V. Ganapathy, M. Thangaraju, P.D. Prasad, Nutrient transporters in cancer: relevance to Warburg hypothesis and beyond, Pharmacol. Ther. 121 (2009) 29–40.
[12] V. Torres-Zamorano, F.H. Leibach, V. Ganapathy, Sodium-dependent homo- and hetero-exchange of neutral amino acids mediated by the amino acid transporter ATB0, Biochem. Biophys. Res. Commun. 245 (1998) 824–829.
[13] N. Utsunomiya-Tate, H. Endou, Y. Kanai, Cloning and functional characterization of a system ASC-like Na+-dependent neutral amino acid transporter, J. Biol. Chem. 271 (1996) 14883–14890.
[14] A. Broer, N. Brookes, V. Ganapathy, K.S. Dimmer, C.A. Wagner, F. Lang, S. Broer, The astroglial ASCT2 amino acid transporter as a mediator of glutamine efflux, J. Neurochem. 73 (1999) 2184–2194.
[15] M. Pollard, D. Meredith, J.D. McGivan, Identification of a plasma membrane glutamine transporter from the rat hepatoma cell line H4-IIE-C3, Biochem. J. 368 (2002) 371–375.
[16] M. Dolinska, B. Zablocka, U. Sonnewald, J. Albrecht, Glutamine uptake and expression of mRNA's of glutamine transporting proteins in mouse cerebellar and cerebral cortical astrocytes and neurons, Neurochem. Int. 44 (2004) 75–81.
[17] F. Oppedisano, L. Pochini, M. Galluccio, M. Cavarelli, C. Indiveri, Reconstitution into liposomes of the glutamine/amino acid transporter from renal cell plasma membrane: functional characterization, kinetics and activation by nucleotides, Biochim. Biophys. Acta 1667 (2004) 122–131.
[18] F. Oppedisano, L. Pochini, M. Galluccio, C. Indiveri, The glutamine/amino acid transporter (ASCT2) reconstituted in liposomes: transport mechanism, regulation by ATP and characterization of the glutamine/glutamate antiport, Biochim. Biophys. Acta 1768 (2007) 291–298.
[19] F. Oppedisano, M. Catto, P.A. Koutentis, O. Nicolotti, L. Pochini, M. Koyioni, A. Introcaso, S.S. Michaelidou, A. Carotti, C. Indiveri, Inactivation of the glutamine/amino acid transporter ASCT2 by 1,2,3-dithiazoles: proteoliposomes as a tool to gain insights in the molecular mechanism of action and of antitumor activity, Toxicol. Appl. Pharmacol. 265 (2012) 93–102.
[20] P.M. Sharp, W.H. Li, The codon adaptation Index—a measure of directional synonymous codon usage bias, and its potential applications, Nucleic Acids Res. 15 (1987) 1281–1295.

[21] F. Oberg, J. Sjohamn, M.T. Conner, R.M. Bill, K. Hedfalk, Improving recombinant eukaryotic membrane protein yields in *Pichia pastoris*: the importance of codon optimization and clone selection, Mol. Membr. Biol. 28 (2011) 398–411.
[22] M. Nyblom, F. Oberg, K. Lindkvist-Petersson, K. Hallgren, H. Findlay, J. Wikstrom, A. Karlsson, O. Hansson, P.J. Booth, R.M. Bill, R. Neutze, K. Hedfalk, Exceptional overproduction of a functional human membrane protein, Protein Expr. Purif. 56 (2007) 110–120.
[23] J. Stratton, V. Chiruvolu, M. Meagher, High cell-density fermentation, Methods Mol. Biol. 103 (1998) 107–120.
[24] M.E. Bushell, M. Rowe, C.A. Avignone-Rossa, J.N. Wardell, Cyclic fed-batch culture for production of human serum albumin in *Pichia pastoris*, Biotechnol. Bioeng. 82 (2003) 678–683.
[25] F. Oberg, J. Sjohamn, G. Fischer, A. Moberg, A. Pedersen, R. Neutze, K. Hedfalk, Glycosylation increases the thermostability of human aquaporin 10 protein, J. Biol. Chem. 286 (2011) 31915–31923.
[26] L. Pochini, M. Scalise, M. Galluccio, L. Amelio, C. Indiveri, Reconstitution in liposomes of the functionally active human OCTN1 (SLC22A4) transporter overexpressed in *Escherichia coli*, Biochem. J. 439 (2011) 227–233.
[27] A. Tonazzi, C. Indiveri, Effects of heavy metal cations on the mitochondrial ornithine/citrulline transporter reconstituted in liposomes, Biometals 24 (2011) 1205–1215.
[28] F. Palmieri, C. Indiveri, F. Bisaccia, V. Iacobazzi, Mitochondrial metabolite carrier proteins: purification, reconstitution, and transport studies, Methods Enzymol. 260 (1995) 349–369.
[29] M. Galluccio, C. Brizio, E.M. Torchetti, P. Ferranti, E. Gianazza, C. Indiveri, M. Barile, Over-expression in *Escherichia coli*, purification and characterization of isoform 2 of human FAD synthetase, Protein Expr. Purif. 52 (2007) 175–181.
[30] A. Sali, T.L. Blundell, Comparative protein modelling by satisfaction of spatial restraints, J. Mol. Biol. 234 (1993) 779–815.
[31] M. Quick, E.M. Wright, Employing *Escherichia coli* to functionally express, purify, and characterize a human transporter, Proc. Natl. Acad. Sci. U. S. A. 99 (2002) 8597–8601.
[32] C. Indiveri, M. Galluccio, M. Scalise, L. Pochini, Strategies of bacterial over expression of membrane transporters relevant in human health: the successful case of the three members of OCTN subfamily, Mol. Biotechnol. 54 (2012) 724–736.
[33] T. Keller, D. Schwarz, F. Bernhard, V. Dotsch, C. Hunte, V. Gorboulev, H. Koepsell, Cell free expression and functional reconstitution of eukaryotic drug transporters, Biochemistry 47 (2008) 4552–4564.
[34] M. Costa, A. Rosell, E. Alvarez-Marimon, A. Zorzano, D. Fotiadis, M. Palacin, Expression of human heteromeric amino acid transporters in the yeast *Pichia pastoris*, Protein Expr. Purif. 87 (2013) 35–40.
[35] M. Galluccio, L. Amelio, M. Scalise, L. Pochini, E. Boles, C. Indiveri, Over-expression in *E. coli* and purification of the human OCTN2 transport protein, Mol. Biotechnol. 50 (2012) 1–7.
[36] M. Scalise, M. Galluccio, L. Pochini, C. Indiveri, Over-expression in *Escherichia coli*, purification and reconstitution in liposomes of the third member of the OCTN sub-family: the mouse carnitine transporter OCTN3, Biochem. Biophys. Res. Commun. 422 (2012) 59–63.
[37] J.W. Deitmer, A. Broer, S. Broer, Glutamine efflux from astrocytes is mediated by multiple pathways, J. Neurochem. 87 (2003) 127–135.
[38] S. Broer, N. Brookes, Transfer of glutamine between astrocytes and neurons, J. Neurochem. 77 (2001) 705–719.
[39] N. Zerangue, M.P. Kavanaugh, ASCT-1 is a neutral amino acid exchanger with chloride channel activity, J. Biol. Chem. 271 (1996) 27991–27994.
[40] L.A. Cynober, Plasma amino acid levels with a note on membrane transport: characteristics, regulation, and metabolic significance, Nutrition 18 (2002) 761–766.
[41] N. Reyes, C. Ginter, O. Boudker, Transport mechanism of a bacterial homologue of glutamate transporters, Nature 462 (2009) 880–885.
[42] C.I. Bungard, J.D. McGivan, Identification of the promoter elements involved in the stimulation of ASCT2 expression by glutamine availability in HepG2 cells and the probable involvement of FXR/RXR dimers, Arch. Biochem. Biophys. 443 (2005) 53–59.
[43] J.S. Amaral, M.J. Pinho, P. Soares-da-Silva, Genomic regulation of intestinal amino acid transporters by aldosterone, Mol. Cell. Biochem. 313 (2008) 1–10.
[44] N.E. Avissar, H.C. Sax, L. Toia, In human entrocytes, GLN transport and ASCT2 surface expression induced by short-term EGF are MAPK, PI3K, and Rho-dependent, Dig. Dis. Sci. 53 (2008) 2113–2125.
[45] M.R. Reynolds, A.N. Lane, B. Robertson, S. Kemp, Y. Liu, B.G. Hill, D.C. Dean, B.F. Clem, Control of glutamine metabolism by the tumor suppressor Rb, Oncogene (2013), http://dx.doi.org/10.1038/onc.2012.635.